water

MDPI

Article

Application of *Klebsiella oxytoca* Biomass in the Biosorptive Treatment of PAH-Bearing Wastewater: Effect of PAH Hydrophobicity and Implications for Prediction

Dong Zhang [1,2], Li Lu [3,*], Hongting Zhao [1], Meiqing Jin [1], Ting Lü [1] and Jun Lin [4]

1 College of Materials and Environmental Engineering, Hangzhou Dianzi University, Hangzhou 310018, China; zhangdong@hdu.edu.cn (D.Z.); hzhao@hdu.edu.cn (H.Z.); jmq@hdu.edu.cn (M.J.); lvting@hdu.edu.cn (T.L.)
2 College of Environmental & Resource Sciences, Zhejiang University, Hangzhou 310058, China
3 School of Environmental Science and Engineering, Zhejiang Gongshang University, Hangzhou 310012, China
4 College of Electronics and Information, Hangzhou Dianzi Univerisity, Hangzhou 310018, China; junlin@hdu.edu.cn
* Correspondence: ll0106@zjgsu.edu.cn; Tel.: +86-571-8500-1993

Received: 4 May 2018; Accepted: 22 May 2018; Published: 24 May 2018

Abstract: Biosorption has been widely recognized as a promising method to treat wastewater. However, few studies have investigated the impact of pollutants' properties on wastewater treatment, as well as the underlying mechanisms and future predictions. In this study, the effects of pollutants' hydrophobicity on the biosorptive removal of polycyclic aromatic hydrocarbons (PAHs) were evaluated. The results showed that the inactive biomass of *Klebsiella oxytoca* effectively removes PAHs from aqueous solutions with a high biosorption capacity, high biosorption affinity, and short equilibrium time. The biosorption of seven PAHs achieved equilibrium rapidly (less than 2 h) and fitted well to the pseudo-second-order kinetic model. Sorption occurred with a predominantly linear partition process to the biomaterial with K_d values of 363.11, 1719.5, 2515.5, 7343.3, 6353.4, 22,806, and 19,541 L·kg^{-1} for naphthalene, acenaphthene, fluorene, phenanthrene, anthracene, pyrene, and fluoranthene, respectively. An increase in temperature led to a decrease in the biosorption affinity, and the bacterial biosorption of PAHs was spontaneous and exothermic. Furthermore, a positive correlation was observed between the sorption affinity and the octanol partition coefficient (K_{ow}) ($\log K_d = 1.011 \log K_{ow} - 0.7369$), indicating that hydrophobicity is the main factor influencing the biosorption efficiency. These results suggest that biosorption is an efficient and predictable treatment for micropollutant-bearing wastewater.

Keywords: biosorption; *Klebsiella oxytoca*; PAHs; partition; prediction

1. Introduction

Hydrophobic organic compounds (HOCs) have become an increasing concern with respect to their potential mutagenicity, carcinogenicity, and teratogenicity associated with their persistence and bioaccumulation potential [1–3]. The adverse impacts on ecosystems and human health caused by specific HOCs, such as polycyclic aromatic hydrocarbon (PAHs) and organic pesticides, have been considered critical problems. In fact, PAHs, such as phenanthrene and pyrene, are recognized as priority micropollutants by the US Environment Protection Agency [4]. To eliminate the impact of such micropollutants, several treatments, namely, combustion, photolysis, sorption, and adding oxidants,

are available [3]. Compared with physical and chemical methods, bioremediation is widely considered to be the most promising and cost-effective approach for the removal of HOCs from contaminated environments and is also relatively efficient [5].

The bioremediation of HOCs is a complex interfacial process, which refers to cell surface sorption, transmembrane processes, and intercellular degradation [5]. Therefore, in the bioremediation process microorganisms play roles as biosorbents that uptake pollutants and bioreactors that degrade them [6]. As one process in bioremediation, biosorption is considered the crucial step and plays a vital role in both the removal and biodegradation of HOCs [1,6–9]. Our previous results indicated that the biosorption of HOCs even governs their biodegradation process due to low bioavailability of HOCs [10]. Microorganisms with higher sorption affinity for organic pollutants may have the advantage of obtaining more "food", resulting in higher biodegradation efficiency, especially for those micropollutants with relatively low water solubility, and thus, bioavailability.

Biosorption is also a branch of biotechnology that effectively reduces chemical concentrations in the aqueous environment using dead or inactive biomass from various origins [11,12]. The application of biosorbents derived from biological materials, such as fungi [2,13–15], bacteria [6,16], and algae [7,17–19], have been extensively examined. Biosorption systems exhibit not only high efficiency but also economic benefits. It was reported that biosorption could reduce the total cost by approximately 28% compared with conventional systems [19,20]. In previous studies, these biomaterials have shown remarkable performance in the biosorption and removal of heavy metals [21–25], dyes [26–28], and pesticides [29,30] due to their high carbon contents, aliphatic and aromatic components, and numerous chemical groups. Many studies have revealed that microbial biomass can passively bind to metal ions, dyes, and some organic antibiotic compounds via various physicochemical mechanisms [19,26,28,31]. These mechanisms include the following: (1) electrostatic attraction [32]; (2) hydrophobic interactions [2,33]; and (3) molecular specific forces, such as n–π interactions [34]. Several studies have indicated that the polarity and aliphatic structures of biosorbents, such as algae and fungi, play important roles in the biosorption of organic pollutants [7,35]. However, the biosorption of HOCs by bacterial biomass and underlying mechanisms has not received much attention. Furthermore, previous studies have mainly focused on the effects of structure, fraction, and modification of biosorbents on the biosorption of HOCs [13]. Limited information about the structural impacts of pollutants and the interaction between pollutant molecules and bacterial biomass is available.

Therefore, the main objectives of this study were to develop a better understanding of the role of biosorption by HOCs in bacterial degradation and treatment of PAH-bearing wastewater, as well as potential future prediction, by the following methods: (1) evaluation of the biosorption, biodegradation, and removal of phenanthrene using *Klebsiella oxytoca*; (2) evaluation of the isotherms, kinetics, and thermodynamics of biosorption of the seven PAHs using inactive biomass of *K. oxytoca*; and (3) examination of the effects of the properties of the PAHs on biosorption.

2. Materials and Methods

2.1. Chemicals

Naphthalene, acenaphthene, fluorene, phenanthrene, anthracene, pyrene, and fluoranthene were selected as representative PAHs to model HOCs and were purchased from Acros Organics (Pittsburgh, PA, USA) with purities >98%. The properties of the seven PAHs are listed in Table 1. All other chemical reagents were of analytical reagent grade.

2.2. Strain, Medium, and Biosorbent

The test bacterial strain *Klebsiella oxytoca* PYR-1 (CCTCC AB 2010358) was isolated from activated sludge of the coking plant wastewater treatment facility and characterized in our previous work [9]. The mineral salt medium (MSM) was composed of (in $mg \cdot L^{-1}$ distilled water) 500 $mg \cdot L^{-1}$ NaH_2PO_4,

850 mg·L^{-1} KH_2PO_4, 1650 mg·L^{-1} K_2HPO_4, 1000 mg·L^{-1} NH_4Cl, 1.0 mg·L^{-1} $MgSO_4{\cdot}7H_2O$, 1.0 mg·L^{-1} $FeSO_4{\cdot}7H_2O$, 0.36 mg·L^{-1} $MnSO_4{\cdot}H_2O$, 0.3 mg·L^{-1} $ZnSO_4{\cdot}7H_2O$, 0.1 mg·L^{-1} $CoCl_2{\cdot}6H_2O$, and 1.0 mg·L^{-1} $CaCl_2{\cdot}2H_2O$. The degradation medium was composed of MSM and phenanthrene (1.0 mg·L^{-1}). MSM-excluded $FeSO_4{\cdot}7H_2O$ was autoclaved at 121 °C for 20 min before use. Phenanthrene and $FeSO_4{\cdot}7H_2O$ were sterilized by vacuum filtration to avoid any transformation of these compounds.

Table 1. Properties and detection of selected polycyclic aromatic hydrocarbons (PAHs).

PAHs	Formula	Molecular Weight	logK_{ow}	S_w, mg·L^{-1}	LOD, μg·L^{-1}	RSD, %
Naphthalene (NAPH)	$C_{10}H_8$	128.2	3.30	31.0	12.2	2.25
Acenaphthene (ACE)	$C_{12}H_{10}$	154.2	3.92	3.90	7.78	0.480
Fluorene (FLU)	$C_{13}H_{10}$	166.2	4.18	1.69	8.45	0.640
Phenanthrene (PHEN)	$C_{14}H_{10}$	178.3	4.46	1.18	3.39	0.230
Anthracene (ANTH)	$C_{14}H_{10}$	178.3	4.45	0.065	0.408	0.235
Pyrene (PYR)	$C_{16}H_{10}$	202.3	4.88	0.12	2.4	0.490
Fluoranthene (FLUOR)	$C_{16}H_{10}$	202.3	5.16	0.26	0.108	0.157

Notes: logK_{ow}, octanol–water partition coefficient; S_w, water solubility at 25 °C; LOD, limit of detection.

Bacterial pellets of *K. oxytoca* PYR-1 were washed three times with deionized water after they had been harvested in the late exponential phase. Inactive biomass, used as a biosorbent, was further prepared by cryodesiccation following mechanical grinding. The specific surface area of the biosorbent was determined by a gas sorption analyzer (NOVA-1200, Quantachrome Corp., Boynton Beach, FL, USA). The biosorbent was further characterized using Fourier transform infrared spectroscopy (FTIR, Shimadzu 8400S, Kyoto, Japan).

2.3. Biodegradation and Sorption of Phenanthrene by a Live Bacterial Strain

The sorption and biodegradation of phenanthrene by *K. oxytoca* PYR-1 were conducted in 500 mL autoclaved Erlenmeyer flasks with 350 mL of autoclaved MSM, as described in our previous work [10], and spiked with phenanthrene at 1.0 mg·L^{-1}. The bacterial strain was inoculated at 5×10^6 CFU·mL^{-1} and incubated at 28 °C in a constant temperature shaker at 150 rpm. Samples were taken every three days. The concentrations of phenanthrene and growth of *K. oxytoca* PYR-1 were measured. The deposits of biomass were ultrasonically extracted with 5.0 mL methanol for 1 h to evaluate the sorption part of phenanthrene, whereas the "real" degraded part was obtained using the mass balance method, as described in our previous work [9]. The apparent removal, sorption, and biodegradation were calculated according to Equations (1)–(3):

$$ARR = (C_0 - C_t - C_{ABL})/C_0 \times 100\%, \quad (1)$$

$$SR = \frac{C_s V_{ex} V_0 / V_{spl}}{C_0 V_0} \times 100\% = \frac{C_s V_{ex} / V_{spl}}{C_0} \times 100\%, \quad (2)$$

$$DR = ARR - SR, \quad (3)$$

where *ARR*, *SR*, and *DR* (%) are the apparent removal ratio, sorption ratio, and biodegradation ratio, respectively. C_0, C_t, and C_s (mg·L^{-1}) are the initial phenanthrene concentration, the phenanthrene concentration of each interval sample and the pellet extraction, respectively. C_{ABL} (mg·L^{-1}) is the concentration of solute abiotic loss measured in the abiotic control. V_{ex} and V_{spl} (mL) are the volumes of extracted methanol and the sample volume, respectively. V_0 (mL) is the initial volume of the solution.

2.4. Biosorption of PAHs by Inactive Bacterial Biomass

Batch sorption experiments were performed in a temperature-controlled shaker at 150 rpm, and tubes were prepared in duplicate. In the kinetic, isotherm, and thermodynamic sorption experiments, two milligrams of inactive biomass were weighed into 22-mL centrifuge tubes with 20 mL of MSM

containing a series of concentrations of seven PAHs (up to their individual water solubility, Table 1). Control treatments without biosorbents were prepared to account for possible solute loss by handling and other possible ways. Single-factor biosorption experiments were also conducted, and other factors were adjusted to suitable conditions as follows: a biosorbent dosage of 0.05–0.4 g·L^{-1}; a biosorption time of 0–720 min; and a sorption temperature of 10–35 °C. The sorption equilibrium time was set up according to the biosorption kinetics experiments. At equilibrium, after being centrifuged for 20 min at 4000 g, the supernatants were filtrated by a 0.22-μm filter membrane (ANPEL Co., Ltd., Shanghai, China).

The biosorption removal of PAHs by the biosorbent was determined using Equation (4):

$$\text{Removal efficiency } (\%) = \left(1 - \frac{C_i}{C_t}\right) \times 100\%, \tag{4}$$

where C_i and C_t (mg·L^{-1}) represent the initial and final (at any time t) concentrations of individual PAHs. The sorption capacity of the biosorbent for PAHs at time t, Q_t (mg·kg^{-1}), was obtained by Equation (5):

$$Q_t = \frac{(C_i - C_t) \times V}{m}, \tag{5}$$

where V (mL) is the volume of the solution, which equaled 20 mL in the present study; and m (mg) represents the mass of the biosorbent.

To determine the sorption kinetics, the obtained dynamic experimental data were fitted with the pseudo-second-order model, which can be written as follows:

$$\frac{t}{Q_t} = \frac{1}{k_2 Q_m^2} + \frac{1}{Q_m} t, \tag{6}$$

where k_2 is the pseudo-second-order rate constant (g·mg^{-1}·min^{-1}); Q_t and Q_m (mg·g^{-1}) are the sorption capacities at time t and equilibrium, respectively. As time approaches zero, according to the pseudo-second-order model, the initial sorption rate (h; mg·g^{-1}·min^{-1}) is calculated as follows:

$$h = k_2 \times Q_m{}^2. \tag{7}$$

The Freundlich model and a linear model were used to describe the isothermal sorption of PAHs by the biosorbent. The logarithmic form of the Freundlich model (original form: $Q_e = K_F \cdot C_e{}^{1/n}$) was used to calculate the Freundlich parameters, and it is expressed in Equation (8):

$$\log Q_e = \log K_F + \frac{1}{n} \log C_e, \tag{8}$$

where Q_e is the amount sorbed per unit weight of sorbent in mg·kg^{-1}; C_e is the equilibrium concentration in mg·L^{-1}; and K_F [(mg·kg^{-1})·(mg·L^{-1})$^{-1}$, equal to L·kg^{-1}] and n (dimensionless) are the Freundlich isotherm constants that describe the sorption capacity and the isotherm curvature, respectively.

The linear isotherm model was also used to estimate the biosorption of PAHs onto the biosorbent. The linear model can be described with the following equation:

$$Q_e = K_d \times C_e, \tag{9}$$

where K_d is the distribution coefficient of sorbate between water and the sorbent in L·kg^{-1}.

The obtained values of K_d under different temperatures were further fitted to the van't Hoff Equation (10):

$$\ln K_d = -\Delta H/(RT) + \Delta S/R, \tag{10}$$

where ΔH and ΔS (kJ·mol^{-1}) are the enthalpy change and entropy change, respectively; R is the universal gas constant (8.314 J^{-1}·mol^{-1}); and T is the absolute temperature (K). When the temperature varied within a narrow range, ΔH and ΔS were regarded as constants and ΔG° (Gibbs free energy change, kJ·mol^{-1}) was calculated with Equation (11) [36]:

$$\Delta G^{\circ} = -RT \ln K_{\mathrm{d}}. \quad (11)$$

2.5. Analytical Methods

The concentrations of PAHs in the aqueous phase were determined using HPLC (Agilent 1200) equipped with a 4.6 × 250 mm Eclipse PAH column and a fluorescence detector using an acetonitrile and water mixture (95:5, V:V) as the mobile phase at a flow rate of 1.0 mL·min^{-1}. The limits of detection and relative standard deviation (RSD) for the seven PAHs were measured and are listed in Table 1.

The biomass of *Klebsiella oxytoca* PYR-1 was measured by a UV-spectrophotometer at 600 nm (UV-2401, Shimadzu Corporation, Kyoto, Japan).

3. Results and Discussion

3.1. Biosorbent Characterization

Figure 1 shows the FTIR spectrum of the biosorbent used in the present study. Several characteristic peaks were identified in the bacterial biomass, and no obvious differences were found in the peak shift upon biosorption of PAHs, e.g., phenanthrene (PHEN). The =C–H stretching of unsaturated hydrocarbons was observed at 980 cm^{-1}. The peak shifts at 1290 cm^{-1} and 1540 cm^{-1} are mainly attributed to the C–O stretching of phenolic compounds and the amide II bond, respectively. The peak near 1650 cm^{-1} denotes the aromatic C=C and C=O asymmetric stretching vibrations [7,35]. A characteristic peak at 1730 cm^{-1} was formed due to the vibration of C=O at the –COOH stretching frequency [37]. The result confirmed that the bacterial surface was abundant in carboxyl, amino groups, saturated and unsaturated aliphatic carbons, and aromatic structures. No obvious differences in biomass composition before and after biosorption were found.

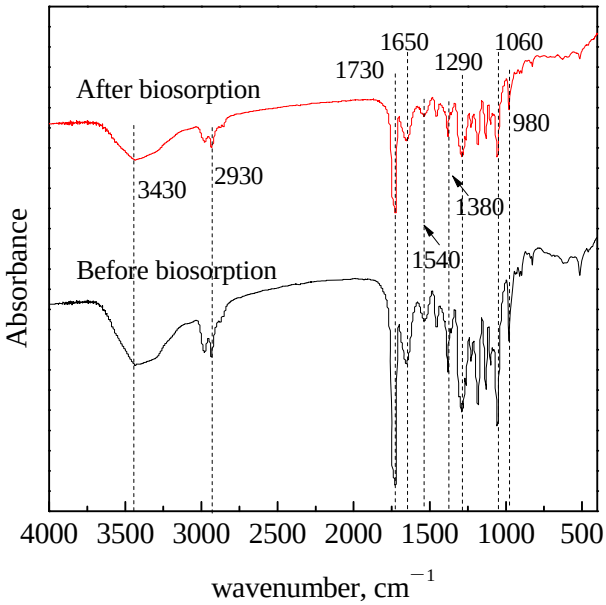

Figure 1. FTIR spectrum of bacterial biomass before and after the biosorption of phenanthrene.

The specific surface area determined by the Brunauer–Emmett–Teller method was 2.34 m^2·g^{-1}, which was quite small but comparable with that used in other studies [38].

3.2. Biosorption and Biodegradation of PHEN by Klebsiella oxytoca PYR-1

The biosorption, biodegradation, and apparent removal of PHEN along with the growth of *K. oxytoca* PYR-1 were measured and distinguished, as shown in Figure 2. The results indicated that the *K. oxytoca* strain could use PHEN as a carbon source and effectively remove up to 68% of PHEN from aqueous solution during the entire incubation period. However, the "real" degradation exhibited a time-delayed phenomenon. Sorption was a relatively fast process due to cell surface adsorption and/or intracellular accumulation [9]. The apparent removal of PHEN was mainly attributed to biosorption, especially in the early phase. For example, biosorption accounted for up to 85.7% of the removed PHEN at day 3, and then, the sorbed PHEN was gradually degraded, resulting in 27.0% biodegradation.

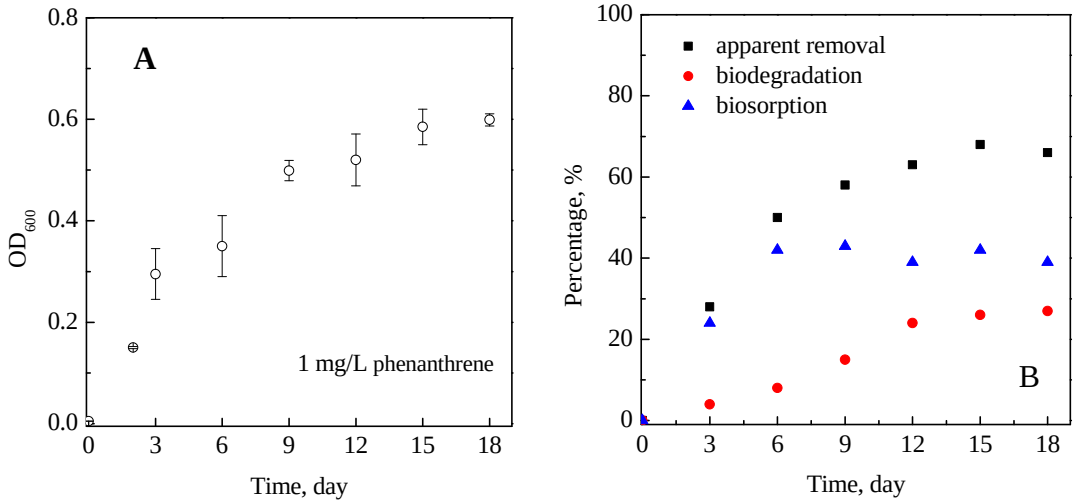

Figure 2. The growth of *Klebsiella oxytoca* with phenanthrene as the sole carbon source (**A**) and the transportation of phenanthrene in water–bacteria system (**B**).

The intracellular, enzyme-assisted degradation of HOCs by bacteria could be recognized as several consecutive interfacial processes, including cell surface biosorption, translocation into the intracellular cytoplasm across the cell membrane, and metabolism and/or accumulation within bacterial cells [5,39]. The bacterial cell surface contains many hydrophobic groups, such as biolipid alkane chains and polysaccharides [34], providing biosorption sites for HOCs. The bacterial cells used in the present work had a relatively high hydrophobicity (21.6%, measured using the bacterial adherence to hydrocarbons method [9]). This high hydrophobicity indicated that the bacterial surfaces had abundant hydrophobic groups, which was confirmed by FTIR measurements (Figure 1). The fast biosorption of PHEN from aqueous solution supplied sufficient substrate for bacterial intracellular enzymes and governed the subsequent biodegradation process [10]. Therefore, the biosorption of HOCs allowed better insight into the interfacial behaviors and mechanisms of bacterial removal of HOCs, as well as a promising treatment of HOCs in the aqueous phase.

3.3. Biosorption of PAHs

3.3.1. Effects of Dosage

Biosorbent dosage is an important factor that plays a role in determining the biosorption capacity and efficiency. In Figure 3, with an increasing dosage (0.05 to 0.4 g·L^{-1}), the biosorption efficiencies for all seven PAHs increased. For example, when the dosage changed from 0.05 g·L^{-1} to 0.4 g·L^{-1}, the removal efficiencies of acenaphthene (ACE), PHEN, and fluoranthene (FLUOR) escalated from

14.4% to 41.3%, 27.3% to 72.6%, and 54.6% to 85.8%, respectively. Similar trends have been reported for metal ions and dyes on several biosorbents [37,38].

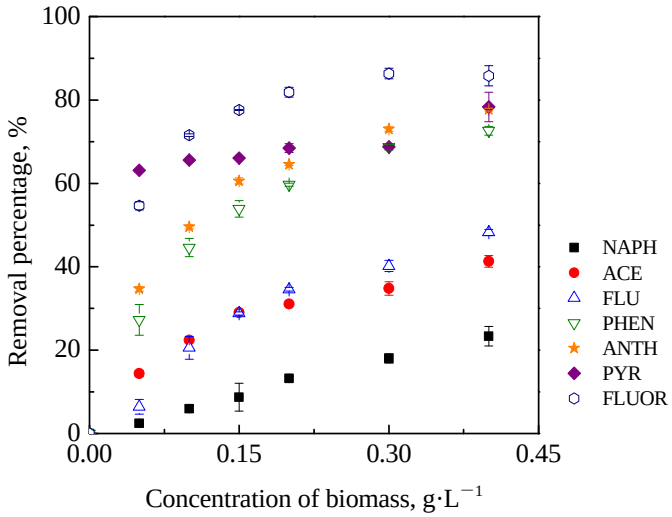

Figure 3. Effects of the biosorbent dosage on the biosorption removal of PAHs.

The biosorption efficiencies were also related to the properties of pollutants, such as hydrophobicity and aromatic rings. With an increase of hydrophobicity (from 3.30 to 5.16 of logK_{ow}), the removal ratio increased. Taking the dosage of 0.2 g·L^{-1} as an example, the removal efficiencies for the seven PAHs were 13.2%, 31.1%, 34.6%, 59.7%, 64.6%, 68.5%, and 81.9% for naphthalene, acenaphthene, fluorene, phenanthrene, anthracene, pyrene, and fluoranthene, respectively.

3.3.2. Biosorption Kinetics

Measurement of the sorption kinetics of the seven PAHs on *Klebsiella oxytoca* PYR-1 biomass was carried out and is presented in Figure 4A. Biphasic biosorption was exhibited for all seven PAHs—a steep initial ascending trend of sorption capacity (Q_t), followed by steady, but slower, accumulation. This phenomenon has been extensively discussed [36]. As shown in Figure 4A, the biosorption equilibrations of all seven PAHs to *K. oxytoca* biomass were achieved in less than 2 h. These equilibrium times are much shorter than those in previously reported studies, e.g., *Microcystis aeruginosa* biomass for PHEN biosorption (more than 24 h) [36], natural and chemically modified biomass of *Phanerochaete chrysosporium* for PHEN biosorption (6 h) [13], and *Typha orientalis* based activated carbon for chloramphenicol biosorption (6 h) [31]. This rapid biosorption is beneficial for further biodegradation as well as for economical and effective engineering applications. Moreover, different sorption capacities were observed on the bacterial biomass for different organic compounds, as follows: naphthalene (NAPH) (6319.5 mg·kg^{-1}), ACE (832.2 mg·kg^{-1}), fluorene (FLU) (964.9 mg·kg^{-1}), PHEN (1407.9 mg·kg^{-1}), anthracene (ANTH) (173.9 mg·kg^{-1}), PYR (584.2 mg·kg^{-1}), and FLUOR (814.4 mg·kg^{-1}). The order of Q_t did not relate to the logK_{ow} of pollutants, mainly because of the dramatic difference in water solubility (Table 1). The biomass in this study showed a higher or comparable sorption capacity to those of reported biosorbents, such as fungal biomass for PHEN (1768.8 mg·kg^{-1}) [13], pinewood for NAPH (2820.6 mg·kg^{-1}) [40], and cork waste for FLU (49 mg·kg^{-1}) and ACE (26 mg·kg^{-1}) [41].

To determine the sorption affinity and suppress the interference of water solubility, a normalized parameter, K_t ($K_t = Q_t/C_t$), was used in the kinetic curves (Figure 4B). It is reasonable that the sorption affinity of the bacterial biomass showed a good relationship with the hydrophobicity of PAHs, with the following ranking: PYR (ca. 26,000 L·kg^{-1}) > FLUOR (11,514 L·kg^{-1}) > ANTH (8751.8 L·kg^{-1}) > PHEN (7352.8 L·kg^{-1}) > ACE (2502.0 L·kg^{-1}) > FLU (1537.9 L·kg^{-1}) > NAPH (355.20 L·kg^{-1}) (Figure 4B).

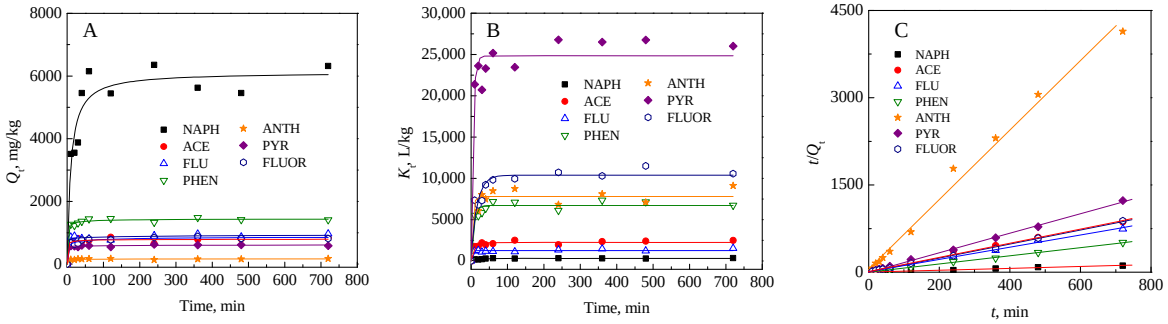

Figure 4. Biosorption kinetics of different PAHs onto inactive biomass. (**A**) biosorption amount; (**B**) normalized parameter K_t with water solubility; (**C**) pseudo-second-order kinetic model.

The biosorption kinetics of all seven PAHs to the biomass of *K. oxytoca* PYR-1 fit well to the pseudo-second-order kinetic model (Figure 4C), and the corresponding parameters (k_2, Q_m, h) and regression coefficients (R^2) are given in Table 2. The calculated values of Q_m based on the pseudo-second-order kinetic model agreed fairly well with the experimental data. The sorption rates (k_2) did not show a strong correlation with the pollutants' hydrophobicity (R^2 = 0.45). However, there was a notable trend for the more hydrophobic PAHs to have a relatively large sorption rate. For example, the k_2 values for PHEN (logK_{ow} 4.46, k_2 0.59152 g·mg^{-1}·min^{-1}) and ACE (logK_{ow} 4.45, k_2 0.61155 g·mg^{-1}·min^{-1}) were much larger than the ones for NAPH (logK_{ow} 3.30, k_2 0.01363 g·mg^{-1}·min^{-1}) and FLU (logK_{ow} 4.18, k_2 0.10715 g·mg^{-1}·min^{-1}). The calculated initial sorption rates (h) were also related to initial concentration and hydrophobicity of PAHs. The higher the initial concentration was, the higher hydrophobicity of PAH was, the larger the h that was obtained. For example, PHEN and FLU had comparable water solubility (1.18 and 1.69 mg·L^{-1}), the h value of PHEN was much larger than that of FLU, following the order of hydrophobicity (4.46 of logK_{ow} for PHEN, 4.18 for FLU).

Table 2. Kinetic parameters for the biosorption of PAHs onto biomass using the pseudo-second order model.

Pseudo-Second Order $t/Q_t = 1/(k_2Q_m^2) + (1/Q_m)t$	k_2, g·mg^{-1}·min^{-1}	Q_m, mg·g^{-1}	h, mg·g^{-1}·min^{-1}	R^2
NAPH	0.01363	6.128	0.5116	0.9916
ACE	0.12781	0.821	0.0862	0.9925
FLU	0.10715	0.951	0.0969	0.9956
PHEN	0.59152	1.418	1.1902	0.9990
ANTH	0.61155	0.168	0.0172	0.9906
PYR	0.22423	1.630	0.5956	0.9986
FLUOR	0.55333	0.829	0.3799	0.9984

3.3.3. Isotherm Biosorption

The biosorption isotherms of the seven PAHs to the biomass of *K. oxytoca* PYR-1 are presented in Figure 5. The isotherms fit well with both the Freundlich model and the linear model, and the parameters are listed in Table 3. An evaluation of the Langmuir model is not reported in this study, due to its poor fit results and the heterogeneous surface of bacterial biomass [34]. The Freundlich exponent n values were approximately 1, and the biosorption isotherms were practically linear. In addition, based on fitness (R^2), the linear model was better for describing the biosorption of PAHs than the Freundlich model. The partition coefficient (K_d) was calculated and is listed in Table 3.

The partition coefficient is a good parameter to evaluate the partitioning of hydrophobic organic pollutants between solid and solution phases. The determined logK_d values were 2.560 for NAPH, 3.235 for ACE, 3.401 for FLU, 3.866 for PHEN, 3.803 for ANTH, 4.358 for PYR, and 4.291 for FLUOR.

These values of inactive biomass were comparable to the values of live cells; for example, the logK_d value was 4.357 for PYR for the live cell of the same *K. oxytoca* strain (data not shown). The results indicate that biosorption might be a useful and convenient practical method for evaluating the sorption process during the biodegradation of HOCs.

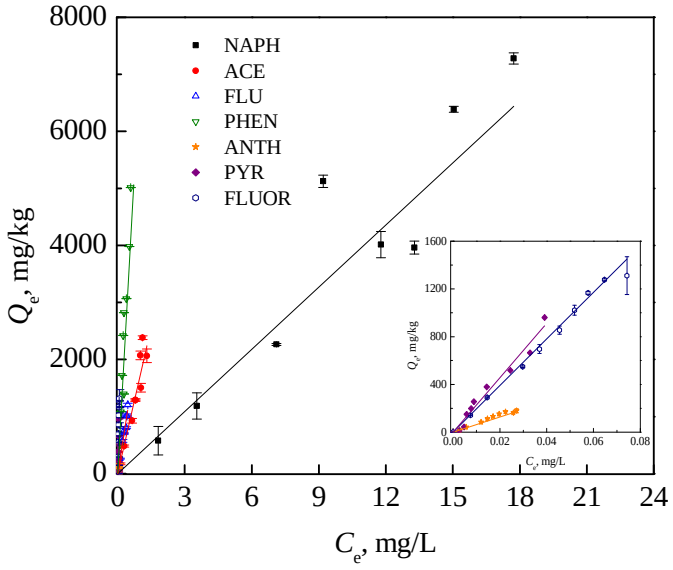

Figure 5. Isothermal biosorption of different PAHs onto inactive biomass.

Table 3. Isothermal parameters of the biosorption of PAHs onto biomass using Freundlich and linear models.

PAHs	Freundlich Model			Linear Model	
	K_F, L·kg^{-1}	n	R^2	K_d, L·kg^{-1}	R^2
NAPH	289.60	0.8883	0.9516	363.11 ± 19.768	0.9711
ACE	1711.2	0.9234	0.9740	1719.5 ± 73.475	0.9820
FLU	2546.2	1.0164	0.9888	2515.5 ± 57.521	0.9948
PHEN	9369.1	0.8774	0.8859	7343.3 ± 641.91	0.9285
ANTH	7174.6	1.0028	0.9890	6353.4 ± 26.720	0.9998
PYR	123,908	0.7014	0.8702	22,806 ± 901.58	0.9846
FLUOR	18,668	1.0077	0.9967	19,541 ± 194.05	0.9990

In addition, by evaluating and comparing the affinity of organic pollutants to biosorbents and/or other solid phases based on the K_d values, the potential transport and fate of these organic contaminants in the environment can be evaluated and predicted. The logK_d values obtained in the present study were much higher than those in the soil–water systems (1.48–2.30) for PHEN [42,43]; higher than those of plant live tissues, such as wood chips (3.40), plant roots (3.32–3.70), plant leaves (3.52–3.54) for PHEN [35] and plant leaves (4.19–4.33) and tissues (4.19–4.33) for PYR [35,44]; higher than those of soil organic matter, such as cellulose and wood fiber for PHEN [35]; and higher than those of algae and planktons (3.36–3.89) for PHEN [35]. In addition, our previous work showed that even in surfactant-containing systems, the biosorption affinity of biomass with PAHs remains high, which facilitates surfactant-enhanced bioremediation [9,10]. For example, in the presence of critical micelle concentrations of Tween 80, Tween 40, Tween 20 and rhamnolipids, the logK_d values for PYR were 4.53, 4.45, 4.47, and 4.35, respectively. Therefore, bacterial biosorption may play an important role in affecting the fate and bioremoval of PAHs in the environment.

A linear correlation was observed between logK_d and logK_{ow} for the tested seven PAHs to the biomass of the *K. oxytoca* strain, as shown in Figure 6:

$$\log K_d = 1.011 \log K_{ow} - 0.7369 \ (n = 7, R^2 = 0.959). \quad (12)$$

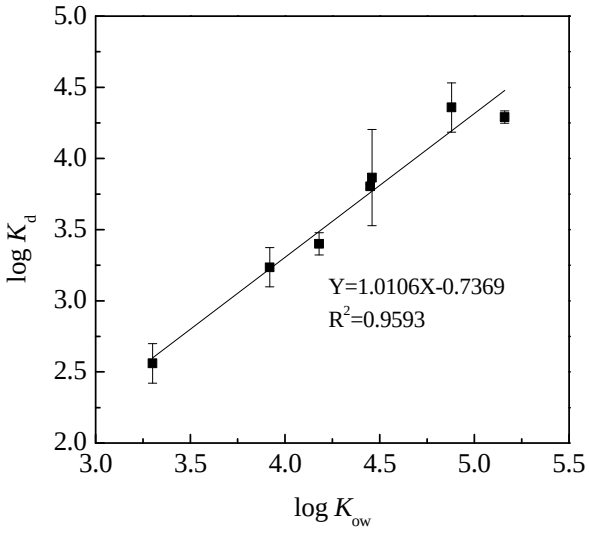

Figure 6. Relationship between the partitioning coefficient (logK_d) and the octanol–water partition coefficient (logK_{ow}) of different PAHs.

According to Equation (12) for logK_d–logK_{ow}, the biosorption of HOCs to bacterial biomass can be predicted. Available sorption data (K_d) of organic compounds to microorganism-derived biosorbents from the literature was compared with predicted K_d values (Table 4). The results revealed that the K_d values predicted by Equation (12) were much closer to the determined values. The results also indicated that this prediction could be used for various hydrophobic organic compounds and microorganism-derived biosorbents.

Table 4. Isothermal parameters of biosorption of PAHs onto biomass using Freundlich and linear models.

Biosorbent	Target Compound	logK_{ow}	Measured K_d, L·kg^{-1}	Predicted K_d, L·kg^{-1}	Prediction Error	Reference
White-rot fungi biomass: *Phanerochaete hrysosporium*	NAPH	3.30	361.0	397.6	10.15	[2]
	ACE	3.92	1656	1684	1.66%	
	FLU	4.18	2890	3084	6.70%	
	PHEN	4.46	6822	5918	13.3%	
	PYR	4.88	24,140	15,732	34.8%	
Mixed bacterial biomass	PHEN	4.46	6340	5918	6.66%	[45]
	PYR	4.88	14,800	15,732	6.30%	
	Benzo[a]pyrene	6.35	450,000	481,892	7.09%	
Brown seaweed biomass: *Sargassum hemiphyllum*	PHEN	4.46	6760	5918	14.2%	[46]
Fungi biomass: *Rhizopus arrhizus*	Lindane	3.72	1057	1170	9.67%	[30]
	Diazinon	3.81	1303	1220	6.82%	
	Pentachlorophenol	5.18	31,629	32,130	1.56%	

3.3.4. Thermodynamic Biosorption

The results showed that all biosorption isotherms of PHEN to *K. oxytoca* biomass were linear at all of the test temperatures (10–35 °C) (data not shown). As shown in Figure 7A, the K_d of PHEN significantly decreased with an increase in temperature, in accordance with other studies [13,47,48]. A positive correlation between lnK_d and 1/T was observed (Figure 7B). The thermodynamic parameters (ΔH, ΔS, as well as $\Delta G°$) were calculated according to Equations (10) and (11). The Gibbs free energy values ($\Delta G°$) were −7.39, −6.02, −5.52, −4.94, −4.84, and −4.88 kJ·mol^{-1} ($\Delta G° < 0$) when the temperature increased from 283 to 308 K. The negative values of $\Delta G°$ indicated that the biosorption of PHEN onto inactive biomass of *K. oxytoca* is a spontaneous process [47]. The standard enthalpy change (ΔH) and standard entropy change (ΔS) were −37.48 and −0.1078 kJ·mol^{-1}, respectively, indicating that the biosorption of PHEN was exothermic [13,48].

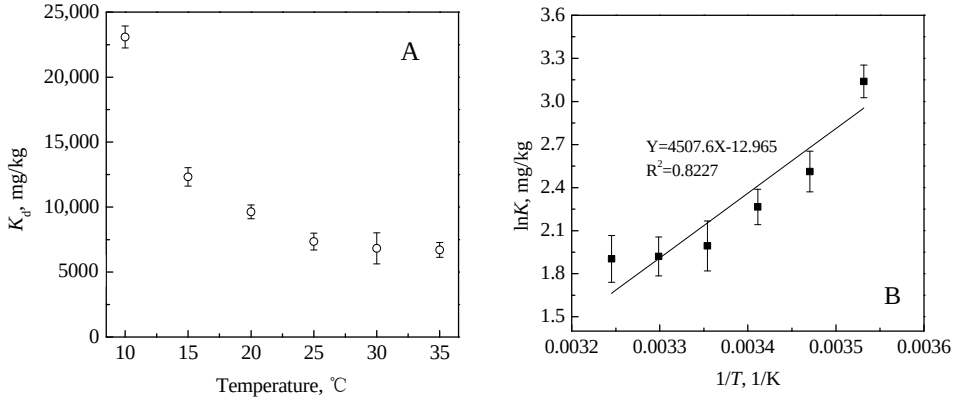

Figure 7. Effects of temperature on the biosorption of phenanthrene onto inactive biomass. (**A**) effects of temperature on partition coefficient; (**B**) relationship between ln$K$ and 1/T.

4. Conclusions

The biomass of *Klebsiella oxytoca* PYR-1 has great potential to remove PAHs via biosorption and biodegradation, with a higher biosorption capacity, shorter equilibrium time, and higher biosorption affinity than other biosorbents. Biosorption played a major role in the bioremoval of PAHs. The biosorption of seven PAHs achieved equilibrium rapidly (in less than 2 h) and fitted well to the pseudo-second-order kinetic model. The biomass exhibited great biosorption capacities for all tested PAHs. For example, relatively large sorption capacities for NAPH (6319.5 mg·kg^{-1}) and FLU (964.9 mg·kg^{-1}) were obtained. Sorption occurred with a predominantly linear partition process to the biomaterial for all seven PAHs. A positive correlation was observed between logK_d and logK_{ow} (logK_d = 1.011logK_{ow} − 0.7369), which could be useful for predicting the biosorption of HOCs to biomasses from different origins. An increase in temperature led to a decrease in biosorption affinity, and the biosorption of PHEN on bacterial biomass was spontaneous and exothermic.

The use of microbial biosorption is a promising alternative to supplement present treatment processes for the removal of high-toxic HOCs from wastewater, facilitating the bioreactor process afterwards. However, the use of biomass to removal organic pollutants is still in the research stage. The prediction for HOC removal by biomass plays an essential role in transferring technology from the laboratory to full-scale application. In this study, we successfully used the relationship logK_d~logK_{ow} to predict the removal of several HOCs. However, to develop a practical prediction, more studies providing sorption parameters, such as sorption affinity (K_d), are needed. Moreover, further investigation for the industrial application of biosorbents (e.g., immobilized biomass beads) is needed.

Author Contributions: Conceptualization, D.Z., L.L. and H.Z.; data curation, M.J. and T.L.; writing original draft, D.Z.; writing, review and editing, L.L., M.J. and J.L.

Funding: This work was supported by the National Natural Science Foundation of China (#21407037, 41301327, 21506045 and 21407038)

Acknowledgments: We are grateful to the anonymous reviewers for their constructive comments and suggestions that greatly improved the manuscript.

Conflicts of Interest: The authors declare no conflict of interest.

References

1. Stringfellow, W.T.; Alvarez-Cohen, L. Evaluating the relationship between the sorption of PAHs to bacterial biomass and biodegradation. *Water Res.* **1999**, *33*, 2535–2544. [CrossRef]
2. Chen, B.L.; Wang, Y.S.; Hu, D.F. Biosorption and biodegradation of polycyclic aromatic hydrocarbons in aqueous solutions by a consortium of white-rot fungi. *J. Hazard. Mater.* **2010**, *179*, 845–851. [CrossRef] [PubMed]
3. Tran, V.S.; Ngo, H.H.; Guo, W.S.; Zhang, J.; Liang, S.; Ton-That, C.; Zhang, X.B. Typical low cost biosorbents for adsorptive removal of specific organic pollutants from water. *Bioresour. Technol.* **2015**, *182*, 353–363. [CrossRef] [PubMed]
4. US EPA (United States Environmental Protection Agency). *Polycyclic Aromatic Hydrocarbons (PAHs)*; Office of Solid Waste: Washington, DC, USA, 2008.
5. Zhang, D.; Zhu, L.Z. Controlling microbiological interfacial behaviors of hydrophobic organic compounds by surfactants in biodegradation process. *Front. Environ. Sci. Eng.* **2014**, *8*, 305–315. [CrossRef]
6. Xu, N.-N.; Bao, M.-T.; Sun, P.-Y.; Li, Y.-M. Study on bioadsorption and biodegradation of petroleum hydrocarbons by a microbial consortium. *Bioresour. Technol.* **2013**, *149*, 22–30. [CrossRef] [PubMed]
7. Zhang, D.-N.; Ran, C.-Y.; Yang, Y.; Ran, Y. Biosorption of phenanthrene by pure algae and field-collected planktons and their fractions. *Chemosphere* **2013**, *93*, 61–68. [CrossRef] [PubMed]
8. Sanches, S.; Marins, M.; Silva, A.F.; Galinha, C.F.; Santos, M.A.; Pereira, I.A.C.; Crespo, M.T.B. Bioremoval of priority polycyclic aromatic hydrocarbons by a microbial community with high sorption ability. *Environ. Sci. Pollut. Res.* **2017**, *24*, 3550–3561. [CrossRef] [PubMed]
9. Zhang, D.; Zhu, L.-Z. Effects of Tween 80 on the removal, sorption and biodegradation of pyrene by *Klebsiealla oxytoca* PYR-1. *Environ. Pollut.* **2012**, *164*, 169–174. [CrossRef] [PubMed]
10. Zhang, D.; Zhu, L.-Z.; Li, F. Influence and mechanisms of surfactants on pyrene biodegradation based on interactions of surfactant with a *Klebsiella oxytoca* strain. *Bioresour. Technol.* **2013**, *142*, 454–461. [CrossRef] [PubMed]
11. Volesky, B. *Sorption and Biosorption*; BV Sorbex: Quebec, QC, Canada, 2003.
12. Aksu, Z. Application of biosorption for the removal of organic pollutants: A review. *Process Biochem.* **2005**, *40*, 997–1026. [CrossRef]
13. Gu, H.-P.; Luo, X.-Y.; Wang, H.-Z.; Wu, L.-S.; Wu, J.-J.; Xu, J.-M. The characteristics of phenanthrene biosorption by chemically modified biomass of *Phanerochaete chrysosporium*. *Environ. Sci. Pollut. Res.* **2015**, *22*, 11850–11861. [CrossRef] [PubMed]
14. Chen, B.-L.; Ding, J. Biosorption and biodegradation of phenanthrene and pyrene in sterilized and unsterilized soil slurry systems stimulated by *Phanerochaete chrysosporium*. *J. Hazard. Mater.* **2012**, *229*, 159–169. [CrossRef] [PubMed]
15. Gu, H.-P.; Luo, J.; Wang, H.-Z.; Yang, Y.; Wu, L.-S.; Wu, J.-J.; Xu, J.-M. Biodegradation, biosorption of phenanthrene and its trans-membrane transport by *Massilia sp* WF1 and *Phanerochaete chrysosporium*. *Front. Microbiol.* **2016**, *7*, 38. [CrossRef] [PubMed]
16. Giri, A.K.; Patel, R.K.; Mahapatra, S.S.; Mishra, P.C. Biosorption of arsenic (III) from aqueous solution by living cells of Bacillus cereus. *Environ. Sci. Pollut. Res.* **2013**, *20*, 1281–1291. [CrossRef] [PubMed]
17. Arias, A.H.; Souissi, A.; Glippa, O.; Roussin, M.; Dumoulin, D.; Net, S.; Ouddane, B.; Souissi, S. Removal and biodegradation of phenanthrene, fluoranthene and pyrene by the marine algae *Rhodomonas baltica* enriched from North Atlantic Coasts. *Bull. Environ. Contam. Toxicol.* **2017**, *98*, 392–399. [CrossRef] [PubMed]
18. Zhang, D.-N.; Ran, Y.; Cao, X.-Y.; Mao, J.-D.; Cui, J.-F.; Schmidt-Rohr, K. Biosorption of nonylphenol by pure algae, field-collected planktons and their fractions. *Environ. Pollut.* **2015**, *198*, 61–69. [CrossRef] [PubMed]

19. Ata, A.; Nalcaci, O.O.; Ovez, B. Macro algae *Gravilaria verrucosa* as a biosorbent: A study of sorption mechanisms. *Algal Res.* **2012**, *1*, 194–204. [CrossRef]
20. Loukidou, M.X.; Zouboulis, A.I.; Karapantsios, T.D.; Matis, K.A. Equilibirum and kinetic modeling of chromium (VI) biosorption by *Aeromonsa caviae*. *Colloid Surf. A* **2004**, *242*, 93–104. [CrossRef]
21. Bano, A.; Hussain, J.; Akbar, A.; Mehmood, K.; Anwar, M.; Hasni, M.S.; Ullah, S.; Sajid, S.; Ali, I. Biosorption of heavy metals by obligate halophilic fungi. *Chemosphere* **2018**, *199*, 218–222. [CrossRef] [PubMed]
22. Park, J.H.; Chon, H.T. Characterization of cadmium biosorption by *Exiguobacterium* sp. Isolated from farmland soil near Cu-Pb-Zn mine. *Environ. Sci. Pollut. Res.* **2016**, *23*, 11814–11822. [CrossRef] [PubMed]
23. Albert, Q.; Leleyter, L.; Lemoine, M.; Heutte, N.; Rioult, J.P.; Sage, L.; Baraud, F.; Garon, D. Comparison of tolerance and biosorption of three trace metals (Cd, Cu, Pb) by soil fungus *Absidia cylindrospora*. *Chemosphere* **2018**, *196*, 386–392. [CrossRef] [PubMed]
24. Yu, Q.; Fein, J.B. Enhanced removal of dissolved Hg(II), Cd(II), and Au(III) from water by *Bacillus subtilis* bacterial biomass containing an elevated concentration of sulfhydryl sites. *Environ. Sci. Technol.* **2017**, *51*, 14360–14367. [CrossRef] [PubMed]
25. Sulaymon, A.H.; Mohammed, A.A.; Al-Musawi, T.J. Competitive biosorption of lead, cadmium, copper, and arsenic ions using algae. *Environ. Sci. Pollut. Res.* **2013**, *20*, 3011–3023. [CrossRef] [PubMed]
26. Cheng, N.; Li, Q.-Y.; Tang, A.-X.; Su, W.; Liu, Y.-Y. Decolorization of a variety of dyes by *Aspergillus flavus* A5p1. *Bioprocess Biosyst. Eng.* **2018**, *41*, 511–518.
27. Zhao, S.-X.; Zhou, T.-S. Biosorption of methylene blue from wastewater by an extraction residue of *Salvia miltiorrhiza* Bge. *Bioresour. Technol.* **2016**, *219*, 330–337. [CrossRef] [PubMed]
28. Chandra, T.S.; Mudliar, S.N.; Vidyashankar, S.; Mukherji, S.; Sarada, R.; Krishnamurthi, K.; Chauhan, V.S. Defatted algal biomass as a non-conventional low-cost adsorbent: Surface characterization and methylene blue adsorption characteristics. *Bioresour. Technol.* **2015**, *184*, 395–404. [CrossRef] [PubMed]
29. Gao, J.; Ye, J.-S.; Ma, J.-W.; Tang, L.-T.; Huang, J. Biosorption and biodegradation of triphenyltin by *Stenotrophomonas maltophilia* and their influence on cellular metabolism. *J. Hazard. Mater.* **2014**, *276*, 112–119. [CrossRef] [PubMed]
30. Tsezos, M.; Bell, J.P. Comparison of the biosorption and desorption of hazardous organic pollutants by live and dead biomass. *Water Res.* **1989**, *23*, 561–568. [CrossRef]
31. Li, Y.-R.; Zhang, J.; Liu, H. Removal of chloramphenicol from aqueous solution using low-cost activated carbon prepared from *Typha orientalis*. *Water* **2018**, *10*, 351.
32. Vijayaraghavan, K.; Yun, Y.-S. Utilization of fermentation waste (*Corynebacterium glutamicum*) for biosorption of Reactive Black 5 from aqueous solution. *J. Hazard. Mater.* **2007**, *141*, 45–52. [CrossRef] [PubMed]
33. Chan, S.M.N.; Luan, T.; Wong, M.H.; Tam, N.F.Y. Removal and biodegradation of polycyclic aromatic hydrocarbons by *Selenastrum capricornutum*. *Environ. Toxicol. Chem.* **2006**, *25*, 1772–1779. [CrossRef] [PubMed]
34. Xiao, L.; Qu, X.; Zhu, D.-Q. Biosorption of nonpolar hydrophobic organic compounds to *Escherichia coli* facilitated by metal and proton surface binding. *Environ. Sci. Technol.* **2007**, *41*, 2750–2755. [CrossRef] [PubMed]
35. Xi, Z.-M.; Chen, B.-L. The effect of structural compositions on the biosorption of phenanthrene and pyrene by tea leaf residues fractions as model biosorbents. *Environ. Sci. Pollut. Res.* **2014**, *21*, 3318–3330. [CrossRef] [PubMed]
36. Bai, L.-L.; Xu, H.-C.; Wang, C.-H.; Deng, J.-C.; Jiang, H.-L. Extracellular polymeric substances facilitate the biosorption of phenanthrene on cyanobacteria *Microcystis aeruginosa*. *Chemosphere* **2016**, *162*, 172–180. [CrossRef] [PubMed]
37. Mahmoud, M.E.; El Zokm, G.E.; Farag, A.E.M.; Abdelwahab, M.S. Assessment of heat-inactivated marine Aspergillus flavus as a novel biosorbent for removal of Cd(II), Hg(II), and Pb(II) from water. *Environ. Sci. Pollut. Res.* **2017**, *24*, 18218–18228. [CrossRef] [PubMed]
38. Puchana-Rosero, M.J.; Lima, E.C.; Ortiz-Monsalve, S.; Mella, B.; Costa, D.; Poll, E.; Gutterres, M. Fungal biomass as biosorbent for the removal of Acid Blue 161 dye in aqueous solution. *Environ. Sci. Pollut. Res.* **2017**, *24*, 4200–4209. [CrossRef] [PubMed]
39. Noinaj, N.; Kuszak, A.J.; Gumbart, J.C.; Lukacik, P.; Chang, H.; Easley, N.C.; Lithgow, T.; Buchanan, S.K. Structural insight into the biogenesis of β-barrel membrane proteins. *Nature* **2013**, *501*, 385–390. [CrossRef] [PubMed]

40. Xi, Z.-M.; Chen, B.-L. Removal of polycyclic aromatic hydrocarbons from aqueous solution by raw and modified plant residue materials as biosorbents. *J. Environ. Sci. (China)* **2014**, *26*, 737–748. [CrossRef]
41. Olivella, M.A.; Jove, P.; Oliveras, A. The use of cork waste as a biosorbent for persistent organic pollutants-study of adsorption/desorption of polycyclic aromatic hydrocarbons. *J. Environ. Sci. Health A* **2011**, *46*, 824–832. [CrossRef] [PubMed]
42. Yang, K.; Zhu, L.-Z.; Xing, B.-S. Enhanced soil washing of phenanthrene by mixed solutions of TX100 and SDBS. *Environ. Sci. Technol.* **2006**, *40*, 4274–7280. [CrossRef] [PubMed]
43. Zhou, W.-J.; Zhu, L.-Z. Enhanced desorption of phenanthrene from contaminated soil using anionic/nonionic mixed surfactant. *Environ. Pollut.* **2007**, *147*, 350–357. [CrossRef] [PubMed]
44. Li, Y.-G.; Chen, B.-L.; Zhu, L.-Z. Enhanced sorption of polycyclic aromatic hydrocarbons from aqueous solution by modified pine bark. *Bioresour. Technol.* **2010**, *101*, 7307–7313. [CrossRef] [PubMed]
45. Steen, W.C.; Karickhoff, S.W. Biosorption of hydrophobic organic pollutants by mixed microbial populations. *Chemosphere* **1984**, *10*, 27–32. [CrossRef]
46. Chung, M.K.; Tsui, M.T.K.; Cheung, K.C.; Tam, N.F.Y.; Wong, M.H. Removal of aqueous phenanthrene by brown seaweed *Sargassum hemiphyllum*: Sorption-kinetic and equilibrium studies. *Sep. Purif. Technol.* **2007**, *54*, 355–362. [CrossRef]
47. Yin, J.; Deng, C.-B.; Yu, Z.; Wang, X.-F.; Xu, G.-P. Effective removal of lead ions from aqueous solution using nano illite/smectite clay: Isotherm, kinetic, and thermodynamic modeling of adsorption. *Water* **2018**, *10*, 210. [CrossRef]
48. Zhang, M.; Ahmad, M.; Lee, S.; Xu, L.; Ok, Y.S. Sorption of polycyclic aromatic hydrocarbons (PAHs) to lignin: Effects of hydrophobicity and temperature. *Bull. Environ. Contam. Toxicol.* **2014**, *93*, 84–88. [CrossRef] [PubMed]